

# Multiple Scattering Calculations for Hydrogen, Helium, Lithium and Beryllium

## Mucool 176

Alvin V. Tollestrup and Jocelyn Monroe

Fermi National Accelerator Laboratory, Box 500, Batavia, Illinois, 60510

The Moliere formalism for multiple scattering of charged particles in various materials requires knowledge of the elastic scattering form factors. The Thomas-Fermi model of the atom is customarily used to obtain these functions. However, this is not accurate for the light elements. The correct form factors for the four lightest elements are given. Heavy beam particles can only be scattered thru a limited angle by the atomic electrons and this modifies the contribution to the scattering process by the atomic electron.

PACS Codes: 25.30.r, 14.60.Ef, 29.17.-a, 41.75.Lx, 41.85.-p

### Introduction

The theory of multiple scattering has a long history, and is usually connected with the early work of Moliere<sup>1</sup>. However, Bethe<sup>2</sup> and later Scott<sup>3</sup> have written extensive papers expanding on Moliere's work. The theory connects the small angle Gaussian like region with the large angle single scattering region and thus covers the plural scattering intermediate region. It is interesting that almost all of this work has been done using the Thomas-Fermi model of the atom to account for the effect the electrons have in shielding the atom. This model is not very accurate for the light elements,  $Z=1$  to  $Z=4$  and we will rectify that defect in what follows. The motivation for this work was inspired by the interest in the possibility of producing and accelerating intense beams of muons for use in a neutrino factory<sup>4</sup> or a muon collider<sup>5</sup>. Since the nuclear interaction of muons is very small, it is possible to damp the random transverse motion in a beam by passing it through a dissipative medium. Hydrogen is the preferred medium since its low  $Z$  minimizes the coulomb scattering, a stochastic process that increases the random transverse motion in the beam.

There is a second effect that needs correction. It is generally assumed that the scattering from the electrons can be included by replacing  $Z^2$  in the Rutherford formula by  $Z(Z+1)$ . This is based on the assumption that the scattering from the electron and the nucleus is the same shape in spite of their enormous mass difference. In the Moliere Theory, the scattering at large angles approaches the Rutherford cross section. However, scattering from electrons is limited kinematically to angles in the laboratory that are less than approximately  $\vartheta_0 = m_e/M$  where  $m_e$  is the electron mass and  $M$  is the mass of the beam particle. Hence if the Gaussian region includes  $\vartheta_0$  (which is 4.8 mr for muons) the asymptotic tail should go as  $Z^2$  not  $Z(Z+1)$ . This particular combination of parameters occurs in a typical muon beam

cooling channel and makes a factor of two difference in the Moliere prediction for the asymptotic hydrogen scattering tail.

This paper will give the correct scattering formulas for H, He, Li and Be using the proper form factors, and will address the problem mentioned in the last paragraph. The work here is based completely on Ref. 2 and equations in that paper will be prefixed with a B before the number, e.g., B1.

### Scattering Cross Section Formulas

The classical Rutherford cross section is given by:

(1)

$$Nt\sigma[\chi] \chi d\chi = 2 \chi_{cl}^2 \chi q[\chi] / \chi^4 d\chi$$

where:

(2)

$$\chi_{cl}^2 = 4 \pi Nt e^4 Z^2 / (p c \beta)^2$$

Nt     The number of atoms/cm<sup>2</sup> in the scattering target,

Z       The charge of the nucleus,

$\beta$       The velocity of the beam particle,

q( $\chi$ )   The form factor of the scattering center,

$\chi_{cl}$     A parameter that defines the target and beam. Note that we have used Z<sup>2</sup> in the definition instead of Z(Z+1) which is used in B10 and we distinguish this by an additional 1 in the subscript.

p       the momentum of the beam particle.

The form factor q( $\chi$ ) in the above expression describes the shielding of the nucleus by the electrons. Since the atom may be left in either its ground state or an excited state, there are two form factors. For the hydrogen atom they can be calculated exactly, and are given by:

(3)

$$q_{el}[t] = (1 - f[t])^2 ; q_{inel}[t] = 1 - f[t]^2$$

$$f[t] = \frac{1}{(1 - a_0^2 t / 4)^2}$$

The variables in the above equations are:

- $a_0$  The Bohr radius in momentum units, 3728 eV/c,
- $t$  the square of the momentum transfer which is approximately  $(p \chi)^2$  for, small scattering angles,
- $q_{el}$  the elastic scattering form factor for the hydrogen atom,
- $q_{inel}$  the inelastic scattering form factor.

These form factors approach 1 for momentum transfers greater than about 25 KeV/c. If they are inserted into Eq.1, it will be seen that the elastic scattering cross section goes to zero at small momentum transfer, but that the inelastic cross section goes to infinity. However, this behavior is cut off by the finite momentum transfer necessary to raise the atom to its first excited state.

For atoms other than hydrogen, we will use the form factors measured by x-ray scattering. Both the elastic and inelastic terms are known for a large variety of elements. The formulas contained in Bethe's article approximate these form factors by using the Thomas-Fermi model for the atom. While this is a good representation for the higher Z elements, it is not so accurate for hydrogen to beryllium. We will give the correct results for these elements using tables for the form factors compiled by Hubbell<sup>6</sup>. The values contained in these tables have been fitted with an interpolation function and are listed in Table 1 in Appendix A.

In order to proceed with the Moliere formalism, we generate a composite form factor by combine the elastic and inelastic scattering:

(4)

$$\sigma[\chi] = 2 \chi_{cl}^2 \left[ \frac{(q_{el}[\chi] + \frac{1}{Z} q_{inel}[\chi])}{(1 + \frac{1}{Z})} \right] \left[ 1 + \frac{1}{Z} \right] / \chi^4$$

(5)

$$\chi_c^2 = \frac{Z+1}{Z} \chi_{c1}^2$$

Since both  $q_{el}$  and  $q_{inel}$  approach one for large  $p$ , one can treat the first term in brackets like a combined form factor that includes both elastic and inelastic scattering. If one notes that our  $\chi_{c1}^2$  includes a factor of  $Z^2$  it becomes apparent that the net factor is  $Z(Z+1)$  which agrees  $\chi_c^2$  with B10. This combined form factor can now be used in the Moliere formulation.

### A Summary of the Formalism.

For convenience, we collect here a brief summary of the formalism contained in Bethe's article. The equation numbers refer directly to the equations in his paper. The scattering is governed by the standard transport equation:

(B1)

$$\partial_t \mathbf{f}[\theta, t] = -N \mathbf{f}[\theta, t] \int \sigma[\chi] \chi d\chi + N \int \mathbf{f}[\theta', t] \sigma[\chi] d\chi$$

$$\vec{\theta}' = \vec{\theta} + \vec{\chi}$$

and is solved by use of a Fourier Bessel Transform:

(B2)

$$\mathbf{f}[\theta, t] = \int_0^\infty \eta J_0[\eta \theta] \mathbf{g}[\eta, t] d\eta$$

(B3)

$$\mathbf{g}[\eta, t] = \int_0^\infty \theta J_0[\eta \theta] \mathbf{f}[\theta, t] d\theta$$

Substitution into (B1) yields an equation that can be immediately integrated for  $\mathbf{g}(\eta, t)$ ;

(B6)

$$\mathbf{g}[\eta, t] = \mathbf{Exp}[-Nt] \int_0^\infty \sigma[\chi] \chi (1 - J_0[\eta \chi]) d\chi$$

Substituting this into (B2) gives the scattering function:

(B7)

$$f[\theta, t] = \int_0^\infty \eta J_0[\theta \eta] \text{Exp}[-Nt \int_0^\infty \sigma[\chi] \chi (1 - J_0[\eta \chi]) d\chi] d\eta$$

Since the cross section is known, integral in the exponential can be evaluated and the scattering determined. This formulation is necessary because the integral for the rms scattering angle is not a stable quantity due to the large tail from the coulomb scattering. The solution of the above equation (B7), joins the Gaussian central core due to multiple scattering and the single coulomb scattering at large angles in a smooth manner.

The solution to (B7) proceeds in two steps. The first involves evaluating the integral in the exponent and is carried out in equations (B11) to (B19). The result is given in terms of a screening angle defined by:

(B16)

$$-\ln[\chi_a] = \lim_{k \rightarrow \infty} \left( \int_0^k q[\chi] / \chi d\chi + \frac{1}{2} - \ln[k] \right)$$

Two additional constants are introduced:

(B19)

$$b = \ln \left[ \frac{\chi_c^2}{\chi_a^2} \right] + 1 - 2 * .577$$

(B23)

$$B - \ln[B] = b$$

The integral in (B7) is then evaluated and yields the following result for the scattering distribution:

(6)

$$f[\theta] \theta d\theta = \frac{\theta d\theta}{B\chi_c^2} \int_0^\infty u J_0 \left[ \frac{u\theta}{\sqrt{B\chi_c^2}} \right] e^{(-\frac{1}{4} u^2 + \frac{1}{4B} u^2 \ln[\frac{1}{4} u^2])} du$$

The quantity B describes the scattering atom through the form factors, and  $\chi_c$  describes the target. B turns out to be a number between 5 and 25 for most of the targets in which we are interested, and so the exponential can be expanded in a power series and the final answer is:

(B25)

$$\mathbf{f}[\theta] \theta d\theta = \frac{\theta d\theta}{B\chi_c^2} \left( \mathbf{f}^{(0)} \left[ \frac{\theta^2}{B\chi_c^2} \right] + \frac{1}{B} \mathbf{f}^{(1)} \left[ \frac{\theta^2}{B\chi_c^2} \right] + \frac{1}{B^2} \dots \dots \right)$$

Where the functions  $\mathbf{f}^{(0)}$  and  $\mathbf{f}^{(1)}$  are given by:

(B27)

$$\mathbf{f}^{(0)}[\mathbf{x}] = 2e^{-\mathbf{x}}$$

(B28)

$$\mathbf{f}^{(1)}[\mathbf{x}] = 2e^{-\mathbf{x}} (\mathbf{x} - 1) (\text{LogIntegral}[e^{\mathbf{x}}] - \ln[\mathbf{x}]) - 2(1 - 2e^{-\mathbf{x}})$$

The first function describes the Gaussian core and the second describes the single scattering tail and is expressed using the LogIntegral function of Mathematica<sup>7</sup>. Higher order terms can be important for small B and can contribute at the several percent level to both the core and the tail. Using Mathematica, it is possible to carry out the numerical integration of (5) directly and compare it with the expansion (B25). Bethe points out that the integral diverges for large values of u, but this is an artifact of the expansion used in evaluating (B6). Empirically, it is found that using an upper limit of 10 in the integral in eq. (5) seems to result in a stable answer.

### The Role of the Electron.

Moliere's development assumes that the scattering cross section for the electron is equal to that of the proton in spite of the large difference in mass. Thus at large angles, the scattering predicted for hydrogen will be double that of the proton alone. However, at large angles the scattering of muons by an electron or by a proton will be very different. In fact the maximum angle for a muon scattered by an electron is given very nearly by

$$(7) \quad \theta_0 = m_e / m_\mu = 4.84 \text{ mr.}$$

This corresponds to  $90^\circ$  scattering in the CM system. If the rms scattering angle is much greater than  $\theta_0$ , then the single scattering tail should not include scattering from the electron and should be proportional to  $Z^2$ , rather than  $Z(Z+1)$ . This effect can be important for cooling a muon beam using hydrogen as an energy loss material and so we have investigated how to correct the Moliere formalism.

The exact scattering cross section in the laboratory system of muons by a proton or an electron is shown for comparison in Fig.1, and it is seen that indeed the scattering at small angles is identical. However, there is a Jacobian singularity at  $90^\circ$  in the cm system and the cross section for scattering by electrons folds back on itself. To a very good approximation they are equal to each other at angles less than  $\theta_0$ . At this point, the cross section has fallen

to such a small value that we will neglect it in what follows. The equality of the small angle cross sections can be easily understood by making a simple impulse calculation of the electron recoil. It is found that the electron moves  $\sim r_e / \beta^2$  during the collision which is negligible for the large impact parameters that are important here.

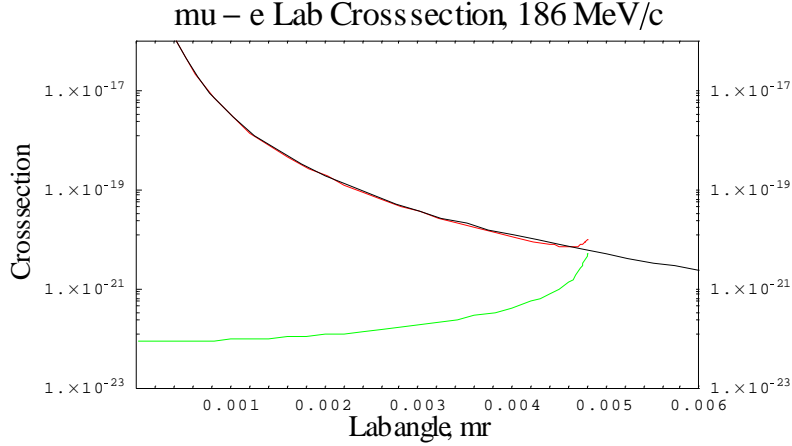


Fig.1 Comparison of mu-e and mu-p coulomb scattering in the laboratory frame. There is a Jacobian peak at an angle corresponding to 90 degrees in the CM system.

The above behavior changes the analysis outlined above. For a pure coulomb scattering process, the rms scattering angle cannot be calculated. The integral diverges at both the upper and lower limit. However, as we have seen, the form factors cutoff the integrand at the lower limit and the Moliere formalism describes the region of plural scattering and matches it on to the single particle scattering from the nucleus and electrons at large angles. If  $\theta_0$  is much smaller than  $\theta_{rms}$  then the electrons will only contribute to the central Gaussian and only the elastic term which is proportional to  $Z^2$  will be left to describe the large angle scattering. This change must be inserted in the evaluation of the integral in the exponent of (B6). The cross section is now written:

(8)

$$\sigma[\chi] = \frac{2 \chi_{cl}^2}{\chi^4} \left( \mathbf{q}_{el}[\chi] + \frac{1}{Z} \mathbf{q}_{inel}[\chi] \right)$$

The integral over the elastic term goes from 0 to infinity as before, however the integral over the inelastic term has an upper limit of  $m_e / m_\mu$ , and so we must evaluate the inelastic term separately. The new set of constants are now defined by:

(9)

$$-\ln[\chi_a^{el}] = \lim_{k \rightarrow \infty} \left( \int_0^k \mathbf{q}^{el}[\chi] / \chi d\chi + \frac{1}{2} - \ln[k] \right)$$

(10)

$$\mathbf{bel} = \int_0^{\theta_0} \frac{\mathbf{q}^{\text{inel}}[\chi]}{\chi} d\chi$$

(11)

$$\mathbf{b}' = \ln\left[\frac{\chi_{\text{cl}}}{\chi_{\text{a}}^{\text{el}}}\right]^2 + 1 - 2 * .577 + \frac{2 * \mathbf{bel}}{\mathbf{z}}$$

(12)

$$\mathbf{B}' - \log[\mathbf{B}'] = \mathbf{b}'$$

(13)

$$\mathbf{f}[\theta] \theta d\theta = \frac{\theta d\theta}{\mathbf{B}' \chi_{\text{cl}}^2} \left( \mathbf{f}^{(0)}\left[\frac{\theta^2}{\mathbf{B}' \chi_{\text{cl}}^2}\right] + \frac{1}{\mathbf{B}'} \mathbf{f}^{(1)}\left[\frac{\theta^2}{\mathbf{B}' \chi_{\text{cl}}^2}\right] + \frac{1}{\mathbf{B}'^2} \dots \dots \right)$$

In this equation, only the elastic scattering from the nucleus contributes to the single scattering tail and although the form is exactly the same as (B25), we have written it out explicitly as the constants are different. Note also the assumption that  $\theta_{\text{rms}} > \theta_0$ .

#### Numerical Details

In the above, we have used angle variables in order to make comparison with Bethe's paper easy. However a much more natural variable is the transverse momentum transfer which is provided by the Coulomb field. Since the angles are small, it is only necessary to multiply each angle variable by  $p$ , the beam momentum, in order to convert the formulas. This removes most of the momentum dependence from the problem, leaving only a  $1/\beta^2$  dependence in the cross section and a linear dependence in the definition of  $\theta_0$ . We will consider first the case where  $\theta_{\text{rms}} < \theta_0$ .

Fig. 2 shows the elastic form factors for H, He, Li, and Be. The hydrogen is calculated using eq(3) and the other three have been obtained from ref.(6). Fig. 3 shows the inelastic form factors. The horizontal scale in each case is eV/c.

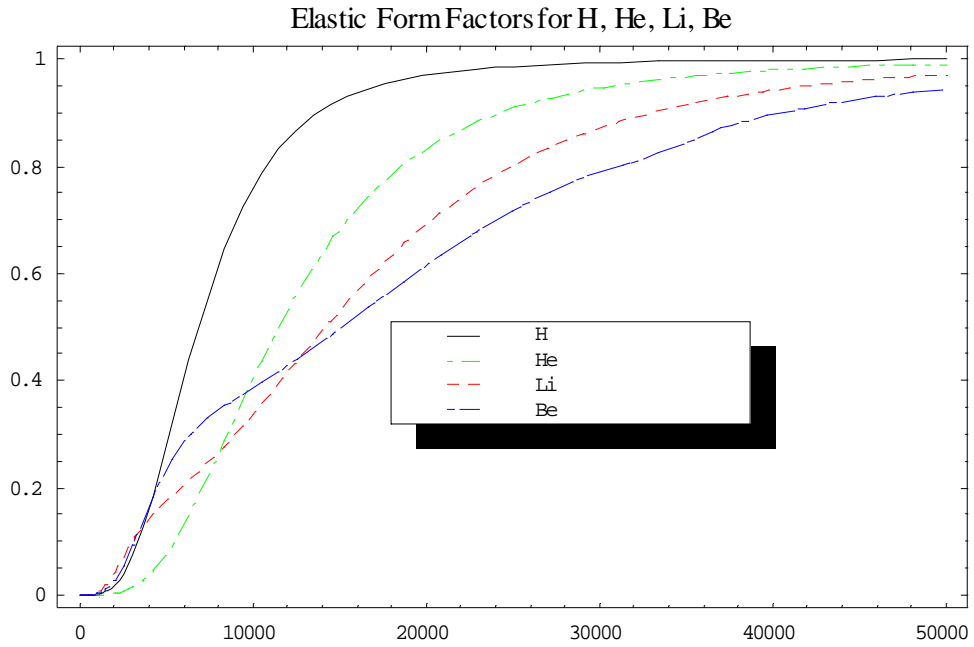


Fig.2. The elastic form factors for H, He, Li, and Be as a function of momentum transfer in units of eV/c.

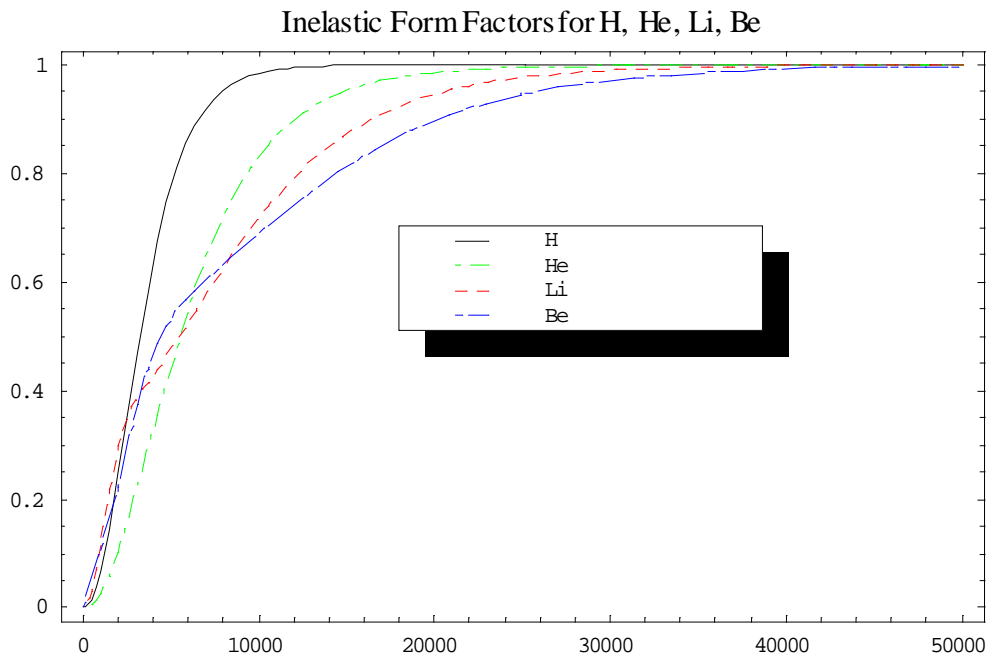


Fig.3. Inelastic form factors for H, He, Li, and Be as a function of momentum transfer in units of eV/c.

Using momentum transfer as a variable, we define the follow quantities in analogy with their corresponding angle variables:

(14)

$$p_c^2 = \frac{4 \pi N t e^4 Z (Z + 1)}{(\beta c)^2}$$

(15)

$$-\ln[p_a] = \lim_{k \rightarrow \infty} \left( \int_0^k q[p_t] / p_t dp_t + \frac{1}{2} - \ln[k] \right)$$

Table 1 lists the above integral over the various form factors form factors:

	H	He	Li	Be
Elastic	4161.76	6977.6	7368.14	7645.22
Inelastic	1808.69	3100.32	2597.54	2946.29

Table 1. Elastic and inelastic  $p_a$  as defined in (14).

We must now combine the elastic and inelastic integrals to define a net shielding  $p_t$  to use in the equation (B25), (see eq.(4) above):

(16)

$$\ln[p_a] = \frac{\ln[p_{aEl}] + \frac{1}{Z} \ln[p_{aInel}]}{1 + \frac{1}{Z}}$$

where:

$p_{aEl}$  = The integral in (14) evaluated with the elastic form factor

$p_{aInel}$  = The integral in (14) evaluated with the inelastic form factor.

The numerical integrals for He, Li and Be have been evaluated in Mathematica using the InterpolationFunctions obtained from the data in Ref(6). The table below compares these sheilding parameters with those obtained using the Thomas-Fermi potential as in (B21).

	H	He	Li	Be
TF values	4493.45	5679.4	6521.89	7200.9
Using FF	2743.6	5324.43	5677.52	6317.82

Table 2. Comparison of the shielding  $p_t$  obtained by using the Thomas-Fermi potential with that obtained by using the correct form factors.

Using the above values of  $p_a$  and  $p_c$  the values of  $b$ , and  $B$  are calculated and used in:

(17)

$$b = \ln\left[\frac{p_c^2}{p_a^2}\right] + 1 - 2 * .577$$

(18)

$$f[p_t] p_t dp_t = \frac{p_t dp_t}{B p_c^2} \left( f^{(0)}\left[\frac{p_t^2}{B p_c^2}\right] + \frac{1}{B} f^{(1)}\left[\frac{p_t^2}{B p_c^2}\right] + \frac{1}{B^2} \dots \dots \right)$$

If  $\theta_{rms} > \theta_0$ , then the above equations must be modified as indicated above. In this case, the integral over the inelastic form factor is limited in angle, or in terms of  $p_t$  to  $p * \theta_0$ . This introduces a momentum dependent term into the value for  $b$  as can be seen in eq.(6). We also must also use  $p_{c1}$  since we want the tail to approach that for a nucleus of charge  $Z$ .

(19)

$$p_{c1}^2 = \frac{4 \pi N t e^4 Z^2}{[c\beta]^2}$$

The term corresponding to  $bel$  in eq.(6) becomes:

(20)

$$bel = \int_1^{10^5} \frac{q[p_t]}{p_t} dp_t + \ln\left[\frac{\theta_0 p}{10^5}\right]$$

(21)

$$b' = \ln\left[\frac{p_{c1}}{p_a^e}\right]^2 + 1 - 2 * .577 + \frac{2 * bel}{Z}$$

The integral in (19) has been evaluated between 1 and  $10^5$  eV/c and is given in Table 3.

H	He	Li	Be
3.51257	2.97368	3.15061	3.0246

Table 3. Values of the integral in (19) for H, He, Li, and Be.

The lower limit is taken as 1 as a simple cutoff for the inelastic scattering. The integral is very insensitive to the value used. The inelastic form factor at  $10^5$  is very close to 1.0, and so the rest of the integral, which depends on angle can be evaluated as a logarithmic term. B is evaluated as before, and distribution is given by:

(22)

$$f[\mathbf{p}_t] p_t dp_t = \frac{p_t dp_t}{B' p_c^2} \left( f^{(0)}[\mathbf{x}] + \frac{1}{B'} f^{(1)}[\mathbf{x}] + \dots \right)$$

where:

(23)

$$\mathbf{x} = \frac{p_t^2}{B' p_{c1}^2}$$

### Examples

Muon cooling channels typically operate with muon momentum near the minimum in the  $dE/dx$  curve at about 200 MeV/c. The length of the absorbers of liquid hydrogen are in the neighborhood of 20 cm long. Such an absorber has an rms scattering angle of a little more than 15 mr, and since this is greater than  $\theta_0$ , it will serve to illustrate some of the features discussed in the previous section. We will use the designations:

PDG	Particle Data Group formula
TF	Thomas Fermi model for the atomic form factors
ZZ	$Z^2$ model for the atom.
ZZ1	$Z(Z+1)$ model.

The constants for the target and beam mentioned above are in Table 4

	PDG	TF	ZZ	ZZ1
$\langle p_t \rangle, \text{MeV}/c$	3.65779	3.44134	3.34293	3.57731
B	na	13.1343	24.7876	14.1927
$pc, \text{eV}/c$	na	949565.	671444.	949565.

Table 4. Scattering constants for a 20 cm liquid hydrogen absorber in a 200 MeV/c muon beam.

The various  $\langle p_t \rangle$  values differ by almost 10%. Both the TF and ZZ1 Models will have a single scattering tail proportional to  $Z(Z+1)=2$  and hence be twice that of the ZZ model. Fig.4 shows the angular distribution of the scattering probability.

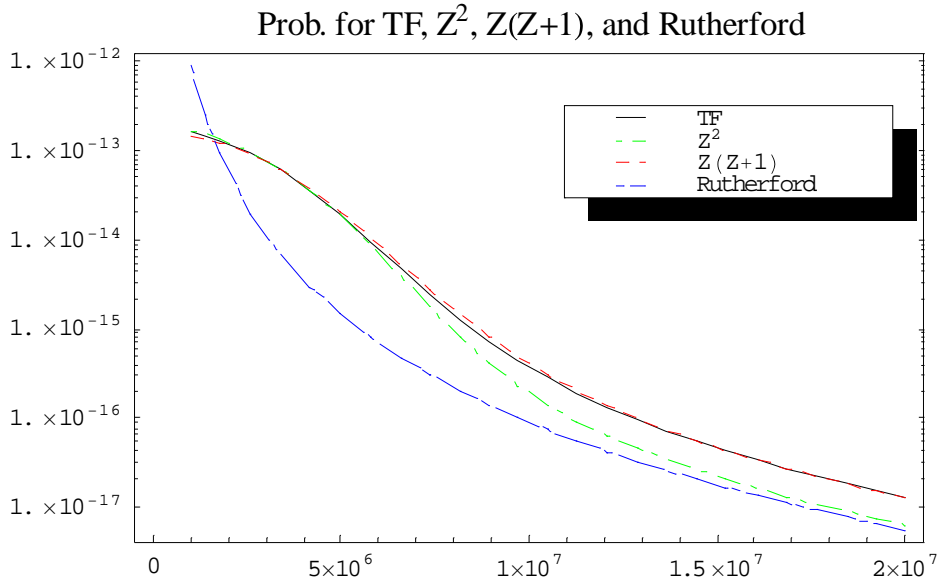


Fig.4. A comparison of the three scattering models along with the single scattering cross section for 20 cm liquid H in a 200 MeV/c beam of muons. Note that the TF and ZZ1 models both are a factor of two higher than the single scattering cross section at large momentum transfers.

The Gaussian width of the curves is about 3.5 MeV/c, and it appears that the scattering probability approaches the single scattering cross section rather slowly. To display the difference between the TF model and the ZZ model, Fig.5 shows the ratio of these two scattering probabilities as a function of  $p_t$ .

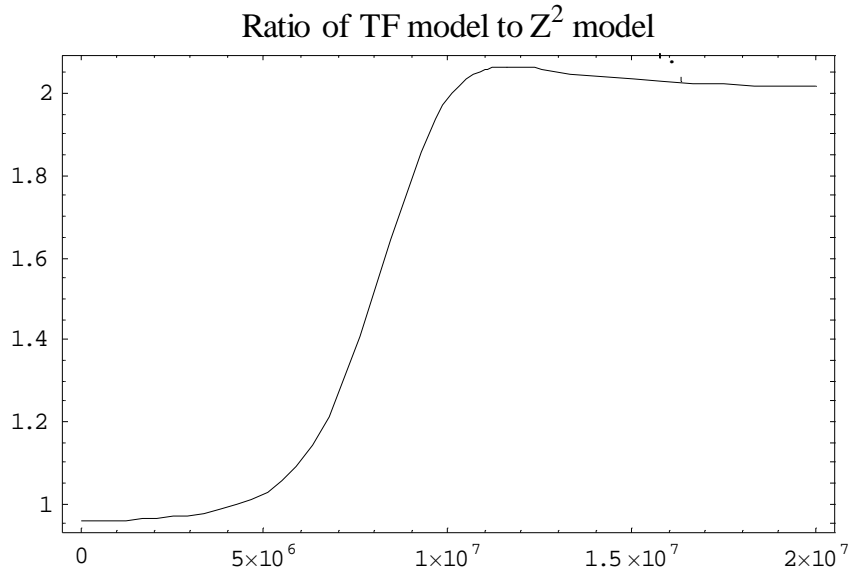


Fig.5. The ratio of the TF model over the ZZ model as a function of  $pt$ .

It is also interesting to investigate the accuracy of using only the first two terms in the expansion (B25). Using Mathematica, a direct integration of eq.(5) with a value for  $B$  of 10 has been carried out. Note that in general  $B$  is larger than 10, and so the error from the third term in the expansion which is proportional to  $B^{-2}$  will be even smaller than what is found here. Fig. 6 shows fractional error in expansion (B25).

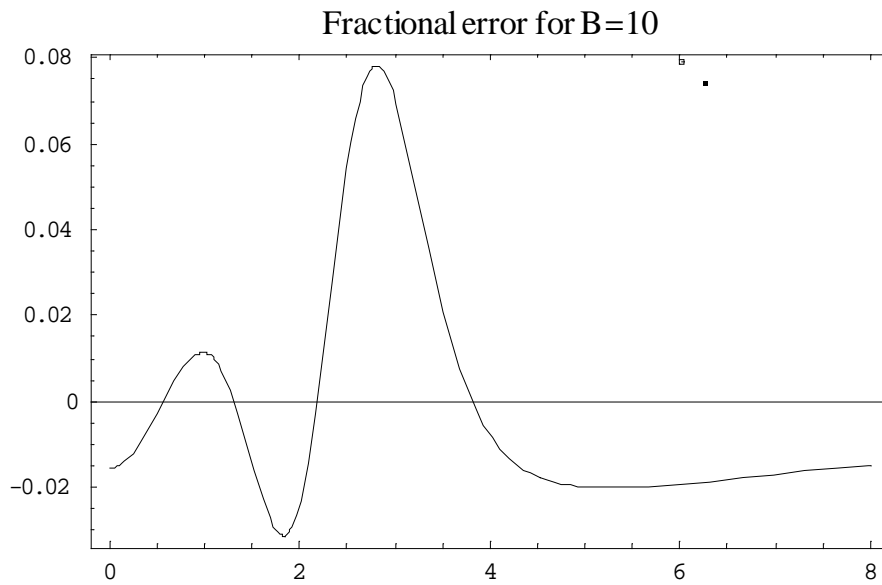


Fig.6 A plot of the fractional error in (B25) vs  $x = pt / (B pc^2)^{1/2}$

A comparison of the above difference with the term  $f^{(2)}$  given in Bethe's paper in Table II shows that this second order term accounts for almost all of the difference.

### Comparison with Experiment

The major difference arising from using the correct form factors instead of the Thomas-Fermi model for the atom should occur for hydrogen. The experiment of Shen<sup>8</sup> et al. measured the multiple scattering in a number of different elements including H, using beams of protons, antiprotons, kaons and pions. The beam momentum was varied between 50 and 200 GeV/c. The data was fit using the Moliere formalism but in all cases using the Thomas-Fermi model of the atom. In order to compare theory and experiment, they express their results in terms of the  $p_t$  that reduces the probability of scattering to 1/e of its central value and they compare this with the value predicted by the Moliere formalism. It is hard to re-evaluate their experiment for the effects of the correct form factors. Since the effect is small, an approximate correction can be made by adjusting for the difference between the computed values of the 1/e angle obtained from the Thomas-Fermi model and that obtained from the model with the correct form factors. The result is given below and is the momentum transfer in MeV/c required to reduce the cross section to 1/e of its value.

Target	Measured Value	TF value	ZZ1 value
Hydrogen	5.42 +/-0.043	5.46	5.686
Beryllium	5.019 +/-0.18	4.93	4.984

The measured value and TF values are taken from Shen's paper. Since the experiment was performed at beam momentum of 50 GeV/c or greater, it is clear that  $\theta_{rms} < \theta_0$  and so the Z(Z+1) model was used for column 4.

An additional correction is necessary when comparing with experiment. The form factor for hydrogen comes from using the atomic wave function, but the molecular effects must be included. The effect is small, and so the correction used here is one calculated for the difference in radiation length caused by the molecular effects<sup>9</sup>. The effect on radiation length involves very similar integrals over momentum transfer to those involved in determining the scattering. The values listed by the PDG<sup>10</sup> are  $X_0 = 63.05$  grms/cm<sup>2</sup> for atomic hydrogen, and 61.28 grms/cm<sup>2</sup> for molecular hydrogen. Molecular hydrogen scatters more than atomic hydrogen by the square root of the ratio of the two radiation lengths, 1.014. Column 4 in the above table has been corrected by this ratio and since this correction was not used in Shen's paper it is not contained in column 3. These corrections to Shen's values should be viewed with caution, as they do not represent a reanalysis of the data.

The cutoff of scattering by the electron has not been measured, as it in general is only important at rather low momentum. This behavior does arise in using a Monte Carlo calculation to model scattering in a thick absorber. The small slices used by the Monte Carlo require the  $Z(Z+1)$  model but with a cutoff for the inelastic term at  $\theta_0$ , but the solution for the whole absorber should be described by the  $Z^2$  model.

### Appendix 1

The following two tables give the interpolated elastic and inelastic form factors for H, He, Li, and Be. The hydrogen values are from the atomic wave function and the others are derived from reference 6.

KeV/c	H	He	Li	Be
0	0	0.	0.	0.
1	0.00122579	0.00019731	0.0043878	0.0021693
2	0.0168174	0.00296658	0.0402034	0.0259832
3	0.0671607	0.0133741	0.0979657	0.0852592
4	0.157525	0.0369671	0.143676	0.163794
5	0.274611	0.0752857	0.177087	0.233889
6	0.398745	0.12784	0.20521	0.285853
7	0.514607	0.191695	0.232322	0.320239
8	0.614344	0.26176	0.264038	0.345281
9	0.695986	0.334019	0.298212	0.365568
10	0.760835	0.404208	0.336369	0.386346
12	0.850759	0.532576	0.415117	0.427279
14	0.904663	0.638399	0.492753	0.472024
16	0.9373	0.721427	0.566959	0.519628
18	0.957528	0.784948	0.634479	0.567828
20	0.970417	0.833107	0.692373	0.614639
22	0.978865	0.869604	0.741815	0.658635
24	0.984551	0.897212	0.783482	0.69911
26	0.988474	0.918205	0.818218	0.735093
28	0.991243	0.934029	0.847101	0.765351
30	0.993236	0.946645	0.871064	0.788816
32	0.994699	0.956635	0.890856	0.808967
34	0.99579	0.963896	0.907111	0.831795
36	0.996616	0.970113	0.920769	0.856754
38	0.997251	0.975711	0.932553	0.880636
40	0.997744	0.979959	0.942497	0.896568
42	0.998132	0.983341	0.950756	0.90974
44	0.998441	0.985977	0.957536	0.92052
46	0.998688	0.987985	0.963044	0.929274
48	0.998889	0.989487	0.967489	0.936369
50	0.999053	0.990722	0.971263	0.942553

Table 5. Elastic form factors for H, He, Li, and Be vs the momentum transfer in KeV/c

KeV/c	H	He	Li	Be
0	0	0.	0.	0.
1	0.0687968	0.0263941	0.119737	0.0674925
2	0.242546	0.100297	0.293405	0.217386
3	0.451147	0.204866	0.384683	0.363757
4	0.636264	0.326799	0.427745	0.467245
5	0.773456	0.445261	0.474665	0.532581
6	0.86418	0.553042	0.524881	0.574883
7	0.920115	0.646624	0.576474	0.60429
8	0.953258	0.722846	0.626745	0.632557
9	0.97253	0.784685	0.674502	0.658884
10	0.983682	0.832129	0.717936	0.688324
12	0.993973	0.899343	0.79285	0.741407
14	0.997613	0.939511	0.850684	0.790035
16	0.998985	0.96321	0.893521	0.832511
18	0.999539	0.977259	0.924389	0.868148
20	0.999778	0.985699	0.946279	0.89715
22	0.999887	0.99088	0.961747	0.920243
24	0.99994	0.994001	0.97257	0.938361
26	0.999967	0.995967	0.980165	0.952384
28	0.999981	0.997073	0.985336	0.963152
30	0.999989	0.997993	0.989269	0.971527
32	0.999993	0.998732	0.992206	0.977954
34	0.999996	0.99898	0.993926	0.982654
36	0.999997	0.999251	0.99542	0.986433
38	0.999998	0.99958	0.99686	0.989671
40	0.999999	0.999734	0.997764	0.992142
42	0.999999	0.99984	0.998413	0.994017
44	0.999999	0.999907	0.998847	0.995384
46	1.	0.999942	0.999107	0.996332
48	1.	0.999953	0.999234	0.996946
50	1.	0.999957	0.999314	0.997406

Table 6. Inelastic form factors for H, He, Li, Be vs the momentum transfer in KeV/c.

## Appendix 2

The above formalism has been installed in DPGEANT for testing, but is not in general use. Shown below is a partial test that was accomplished by artificially restricting the step size in the program to 0.4 cm. Normally, DPGEANT chooses the step size to fit the changing conditions. The muon momentum was chosen to be 184 MeV/c, and good agreement was obtained between the Monte Carlo and the ZZ1 analytical prediction for hydrogen slab 0.4 cm thick. This step verified that we had installed the above theory correctly into the

program. Next using the fixed step size, the program was run for a 32 cm thick target and the results compared with the ZZ1 analytical prediction.

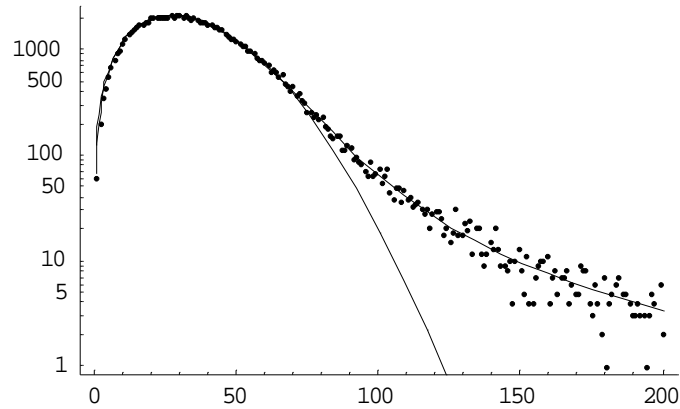


Figure 7. DPGEANT Monte Carlo prediction for 184 MeV/c muon scattering in a 32 cm thick Hydrogen absorber. The horizontal scale is histogram bins with maximum angle of 100 mr. The curve through the data is the normalized Moliere shape, and the lower curve the Gaussian central core for comparison.

It is seen that the Monte Carlo is modeling the theory well. However, more work needs to be done. For the 32 cm absorber,  $\theta_{rms} < \theta_0$  and hence the ZZ prediction should be used to get the single scattering tail. The correct procedure would be to install a cutoff on the inelastic scattering cross section for angles greater than  $\theta_0$  in the ZZ1 model which is correctly used for the 4 mm steps. And then demonstrate that the Monte Carlo prediction for the 32 cm absorber is equal to the analytical prediction form the ZZ model.

---

<sup>1</sup> G. Moliere, Z. Naturforsch **3a**, p. 78 (1948). (In print)

<sup>2</sup> H. A. Bethe, Physical Review **89**, p. 1256 (1953). (In print)

<sup>3</sup> William T. Scott, Review of Modern Physics **35**, p. 231 (1963). (In print)

<sup>4</sup> N. Holtkmap and D. Finley, A Feasibility Study of a Neutrino Source Based on a Muon Storage Ring, Fermi National Accelerator Laboratory, FERMILAB-PUB-00-108-E (2000).(to be published).

<sup>5</sup> Charles M. Ankenbrandt , Muzaffer Atac and et. al., Phys. Rev. ST Accel. Beams **2**, p. 081001 (1999). (In print)

<sup>6</sup> J. H. Hubbell and et al., J. Phys. Chem. Ref.Data, **4**, No.3 (1975). (In print)

<sup>7</sup> Mathematica Version 4.0 Wolfram Research

<sup>8</sup> G. Shen, C. Ankenbrandt and et al., Physical Review D **20**, p. 1584 (1979). (In print)

---

<sup>9</sup> D. Bernstein and W. K. H. Panofsky, Physical Review 102, p. 522 (1956). (In print)

<sup>10</sup> Particle Data Group, D.E. Groom and et al, The European Physical Journal C15, (2000).  
(In Print)